

The Discovery of Macrocyclic XIAP Antagonists from a DNA-Programmed Chemistry Library, and Their Optimization To Give Lead Compounds with in Vivo Antitumor Activity

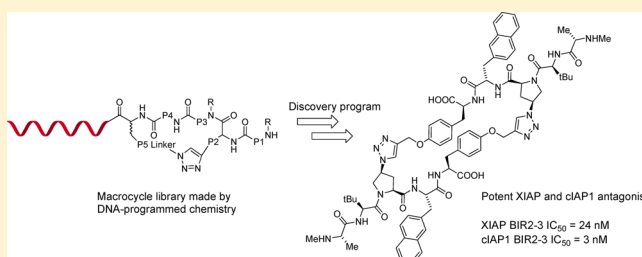
Benjamin A. Seigal,[†] William H. Connors,[†] Andrew Fraley,[†] Robert M. Borzilleri,[‡] Percy H. Carter,[‡] Stuart L. Emanuel,[‡] Joseph Fagnoli,[‡] Kyoung Kim,[‡] Ming Lei,[‡] Joseph G. Naglich,[‡] Matthew E. Pokross,[‡] Shana L. Posy,[‡] Henry Shen,[‡] Neha Surti,[‡] Randy Talbott,[‡] Yong Zhang,[‡] and Nicholas K. Terrett*,[†]

[†]Ensemble Therapeutics Corp, 99 Erie Street, Cambridge, Massachusetts 02139, United States

[‡]Bristol-Myers Squibb Research & Development, P.O. Box 4000, Princeton, New Jersey 08543, United States

S Supporting Information

ABSTRACT: Affinity selection screening of macrocycle libraries derived from DNA-programmed chemistry identified XIAP BIR2 and BIR3 domain inhibitors that displace bound pro-apoptotic caspases. X-ray cocrystal structures of key compounds with XIAP BIR2 suggested potency-enhancing structural modifications. Optimization of dimeric macrocycles with similar affinity for both domains were potent pro-apoptotic agents in cancer cell lines and efficacious in shrinking tumors in a mouse xenograft model.



INTRODUCTION

Failure of cells to execute programmed cell death (PCD), or apoptosis, is a hallmark of many disorders including cancer.¹ Central to PCD is activation of initiator and effector caspases, cysteine proteases that degrade intracellular proteins to begin cell dismantling.^{2,3} Two routes of PCD, the extrinsic and intrinsic pathways, differ in the initiator caspases utilized but converge by activating common effector caspases. Tumor cells have developed several mechanisms to blunt PCD including inhibitor of apoptosis (IAP) regulatory proteins,⁴ which inhibit caspases either by interacting with upstream molecular components or by direct binding. Cellular inhibitor of apoptosis proteins (cIAPs) inhibit the extrinsic pathway by reducing levels of activated initiator caspase-8 protein. X-Chromosome-linked inhibitor of apoptosis protein (XIAP) directly binds and inhibits the activation of initiator and effector caspases common to both apoptotic pathways. Increased XIAP expression often correlates with poor clinical outcomes in cancer treatment, and XIAP deregulation has been implicated in a variety of disorders including neurodegeneration, cancer, and autoimmune disorders.⁵

cIAPs and XIAP contain three segments designated as baculovirus IAP repeat (BIR1–3) domains.⁶ While cIAPs can bind caspases in vitro, their inhibitory activity stems from the ability to block extrinsic caspase activation.⁷ The natural inhibitor of IAPs is the mitochondrial-derived Smac protein which binds through the N-terminal tetrapeptide, AVPI, an attractive starting point for novel inhibitor design.⁸ Several pharmaceutical companies specifically target the IAP BIR3 domain: for example Ascenta/Debiopharm,⁹ Novartis,¹⁰ and Genentech¹¹ have identified monomeric Smac mimetics (SMs) for clinical develop-

ment. These small molecule SMs have been shown to bind tightly to the BIR3 pocket of cIAP. Tumor cells that initiate PCD in response to treatments targeting the BIR3 domain¹² of cIAPs such as MDA-MB-231 triple negative breast cancer are said to undergo type I apoptosis. Conversely, XIAP is a potent inhibitor of both initiator and effector caspases. XIAP BIR3 domain binds initiator caspase-9 and prevents catalytically active dimer formation. XIAP directly inhibits effector caspases tethered to its BIR2 domain, promoting the interaction of an unstructured linker region immediately preceding the domain to block executioner caspase catalytic sites.¹³ XIAP can thus interfere with both the intrinsic and extrinsic pathways of caspase activation to inhibit PCD. Tumor cells that do not respond to elevated caspase-8 levels alone require treatment with dimeric SMs that bind the cIAP BIR3 domain to increase caspase-8 levels and both domains of XIAP to facilitate inhibition of its anticaspase-3 activity. For example, the A875 melanoma line requires XIAP inhibition to complete PCD and is characterized as undergoing type II apoptosis.¹⁴ Therefore, compounds that target both domains rather than just one are attractive as they release both intrinsic and extrinsic caspase pathway inhibition (vida supra). TetraLogic,¹⁵ Human Genome Sciences,¹⁶ and AstraZeneca¹⁷ have described dimeric SMs targeting BIR2 and BIR3 domains of XIAP.

Our search for cIAP/XIAP antagonists arose both from the clinical relevance of the target and an opportunity to exploit macrocycle libraries for novel lead discovery. Several studies have pointed to the benefits of macrocycles as unique binding motifs

Received: December 5, 2014

Published: February 19, 2015

for disrupting protein–protein interactions.¹⁸ Macrocycles demonstrate several advantages not inherent in traditional small molecule drugs, including conformational rigidity, propensity for reducing polar surface area through intramolecular hydrogen bonding, extended interaction motifs, and resistance to metabolic degradation.

It has been established that DNA-encoded small molecules with binding affinity for target proteins can be enriched from complex library mixtures.^{19,20} DNA-programmed chemistry (DPC) is a method for directly translating DNA sequences into small molecules and can be applied in parallel within mixtures to generate large libraries for drug discovery.^{21,22} We have developed extensive libraries of DNA-encoded macrocycles using the specificity and high-throughput synthetic capacity of DPC. In this study, DPC methods permitted the identification of novel macrocycles with high affinity for both the BIR2 and BIR3 domains of XIAP.

RESULTS AND DISCUSSION

DPC Macrocycle Library. We designed a DNA-programmed library (codename ELC) of 160000 cyclic peptidomimetics (Figure 1) that contained a basic *N*-terminal P1 amino

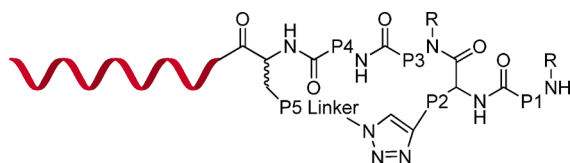


Figure 1. Generic structure of macrocyclic compounds in the DPC-generated ELC library.

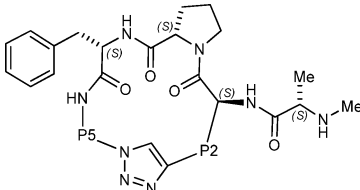
acid in direct mimicry of alanine in the Smac P1 position. The library contained 20 diverse amino acid building blocks in each of positions P1, P3, and P4 that included but were not restricted to natural α -amino acids. The library also incorporated five so-called “linker” azido-substituted amino acids in the P5 position that permitted covalent attachment to the DNA encoding template. The macrocycle ring was completed by Huisgen 1,3-dipolar cycloaddition of the P5 azide onto an alkyne side chain of the P2 amino acid to give cyclic products containing a 1,2,3-triazole ring. Four different alkynes were selected for the P2 position, one for each of four library mixtures (ELC1 through ELC4) generating 40000 variants giving a total library diversity of 160000 ($20 \times 20 \times 20 \times 5 \times 4$) macrocycles.

The pentapeptide was synthesized on DNA using the DPC method as described by Gartner et al.,²⁰ with a final cyclization via triazole formation under Huisgen conditions. Each of the four library mixtures was screened independently against isolated immobilized human XIAP BIR2 and BIR3 domains. Unlike traditional HTS, each 40000 compound mixture could be screened as one entity, removing the need for intensive screening automation. Following incubation of the DNA-labeled library with the target protein immobilized on solid support (biotinylated BIR2 on streptavidin resin and his-tagged BIR3 on nickel resin), nonbinding conjugated macrocycles were washed from the protein. Bound macrocyclic library members were subsequently collected by denaturing the protein by washing the resin with TBST buffer at 70 °C. To identify the hit macrocycles, DNA template sequences were amplified by PCR and sequenced to provide compound binding data. As the quantity of each library member was represented in unequal abundance, selection results were interpreted based on the ratio of the frequency of an individual DNA sequence as a proportion of the total DNA library compared with its abundance in the preselection population.

P2–P5 Linked Macrocycles. Through the screening process, a number of highly enriched template sequences were observed, albeit only from selections undertaken against the XIAP-BIR3 domain target. DNA template sequences translated directly to the structure of specific P2–P5 linked macrocycles synthesized as a consequence of specific codon–anticodon base pairing during DPC. The most enriched sequences were observed in libraries ELC1 and ELC2, which corresponded to compounds prepared from *L*-propynylglycine (ELC1) or *L*-*N*-(pent-4-ynoyl)lysine (ELC2) in the P2 position (see Table 1). From enrichments observed from ELC1 and ELC2 libraries, there was an overwhelming preference for *L*-*N*-methylalanine in the P1 position, with *L*-alanine observed in a few less strongly enriched DNA sequences. *L*-Proline was unequivocally the most preferred P3 residue, and *L*-phenylalanine was highly preferred in the P4 position. These amino acid preferences were not surprising given that the *N*-terminal sequence of Smac is Ala-Val-Pro-Ile-Ala-. In the P5 position, the residue which provided the azide for macrocyclic closure by Click chemistry onto the P2 alkyne, there was no particular preference, although a tertiary amine-containing glycine derivative as found in 4 was implicated by many enriched DNA sequences.

The activity and SAR of novel macrocyclic XIAP-BIR3 binders was confirmed by screening macrocycles prepared by conven-

Table 1. Binding Affinities (IC_{50} values) of P2–P5 Linked Macrocyclic Compounds for XIAP BIR2 and BIR3



compd	P2	P5	XIAP BIR2 IC_{50} (μ M)	XIAP BIR3 IC_{50} (μ M)
1	CH ₂	L-CH(COOH)CH ₂ (C ₆ H ₄)O(CH ₂) ₂	>18.8	1.32
2	(CH ₂) ₄ NHCO(CH ₂) ₂	L-CH(COOH)CH ₂ (C ₆ H ₄)O(CH ₂) ₂	>18.8	1.49
3	(CH ₂) ₄ NHCO(CH ₂) ₂	L-CH(COOH)(CH ₂) ₄	>18.8	1.36
4	(CH ₂) ₄ NHCO(CH ₂) ₂	(CH ₂) ₂ N(CH ₂ COOH)(CH ₂) ₂	>18.8	0.90
5	CH ₂ (C ₆ H ₄)OCH ₂	L-CH(COOH)CH ₂ (C ₆ H ₄)O(CH ₂) ₃	4.87	0.366
6	CH ₂ (C ₆ H ₄)OCH ₂	D-CH(COOH)CH ₂ (C ₆ H ₄)O(CH ₂) ₂	7.99	2.88

tional synthesis. Compounds were made as linear precursors on solid-phase support and cyclized by Huisgen 1,3-dipolar cycloaddition reactions (see Experimental Section below). As the individual molecule products no longer required a linker to DNA, the P5 building block instead contained a carboxylic acid substituent.

The P2–P5 cyclized compounds prepared and their binding data are listed in Table 1 (1–4). Among the most enriched compounds were 1 and 2, prepared in the ELC1 and ELC2 libraries, respectively. These compounds reveal a strong preference for P1 *L*-N-methylalanine, P3 *L*-proline, and P4 *L*-Phe, but the variation in the P2 and P5 residues suggests a less strict requirement for ring size and conformation. Compounds were screened in a fluorescence polarization assay (FPA) for XIAP-BIR3 and an alpha screen assay for XIAP-BIR2 (insufficient signal from binding BIR2 was detected in a FPA format), and these two examples revealed IC_{50} values in the low micromolar range against BIR3 but greater than 18.8 μ M (the highest concentration tested) against BIR2.

Iterative Macrocycle Library. Following discovery of micromolar inhibitory compounds against XIAP-BIR3, an iterative library, designated ELC_{IT}, was prepared to find more potent compounds ideally with inhibitory activity against both BIR domains. There was not significant structural variation introduced among the 1760 compounds prepared in this library, as the aim was to explore SAR close to the preliminary hit structures. The new library compounds, mixed with 40000 compounds from the ELC1 library, were screened in an affinity selection assay. Combining libraries was beneficial in a competition assay format so as to “dilute” the likely many new binding compounds with large numbers of inactive compounds from ELC1 to give more significant DNA sequence enrichment. Furthermore, several of the active compounds in ELC1 would provide a benchmark level of activity against which new hits could be compared.

Following analysis of enriched DNA sequences identified from this affinity selection assay, we observed that ELC_{IT} contained hits with affinity for both BIR2 and BIR3 protein domains. Several compounds were selected for conventional synthesis and inhibitory activity against both domains was assessed. The presence of a P2 tyrosine derivative in the backbone of the macrocycle (e.g., 5 and 6) appeared to be a key feature in compounds that bound to both targets (see Table 1). Results also indicated that the stereochemistry of the P5 residue was not a significant influence on inhibitory activity against either domain.

Monomeric P3–P5 Macrocycles. Co-crystal structures of key compounds bound to the isolated XIAP-BIR2 domain were highly revealing of the bound conformation of macrocycles (Figure 2a). When in complex with BIR2, the peptide backbone of 5 makes numerous hydrogen-bonding interactions with the protein. There are several lipophilic pockets on the protein surface, which are occupied by the P1 methyl side chain and the P4 phenylalanine side chain in particular, but it is noticeable that the P2 and P5 groups constituting the macrocycle backbone are oriented largely into solvent.

For comparison, we examined the binding of an open-chain peptidomimetic analogue 7 (Figure 2c), with a P2 propynyl side chain and an *O*-(2-azidoethyl)tyrosine in P5, the synthetic precursor to the macrocycle compound 1. It was found to interact with the BIR2 protein domain in a very similar manner to 5. The compound has good affinity for both the BIR2 and BIR3 domains (IC_{50} values of 540 and 180 nM, respectively), demonstrating affinity that far exceeds that of macrocycle 1. More revealing is the

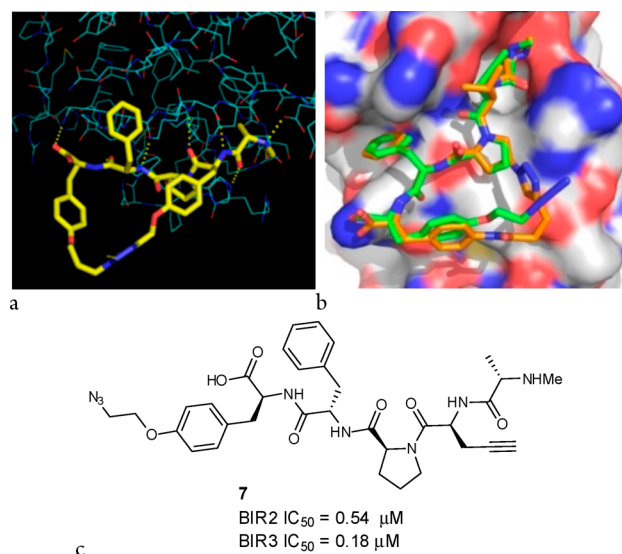


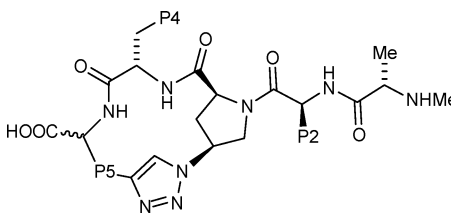
Figure 2. X-ray cocrystal structural information indicated a superior macrocyclic ring closure resulting in a series of compounds with greater binding affinity for the XIAP BIR2 binding site (a) X-ray cocrystal structure of the P2–P5 linked macrocycle 5 (yellow) bound to the BIR2 domain (PDB 4WVT). The compound makes a number of hydrogen-bond interactions (indicated as yellow broken lines) and lipophilic interactions from the P1, P3, and P4 side chains. (b) Overlap of the cocrystal structures of the BIR2 domain with the linear 7 (green) (PDB 4WVS) and P3–P5 linked macrocycle 8 (orange) (PDB 4WVU) showing that the backbone of the open chain overlaps almost exactly with the P3–P5 linked macrocycle 8. (c) Structure of 7, linear precursor to macrocycle 1, a P2–P5 linked macrocycle.

observation that the 4-substituent on the tyrosine side chain is in close proximity through space to the P3 proline group rather than being adjacent to the P2 side chain. This suggests that macrocycles linked between the P3 and P5 side chains might be superior binders, at least to the XIAP BIR2 domain. A similar consideration of the cocrystal structure of an open chain peptidomimetic has been successfully used in the design of macrocycle inhibitors of hepatitis C virus NS3 protease.²³

Following this insight, a number of macrocycles were prepared by reacting a P5 alkyne side chain with *L*-4-(*S*)-azidoproline to give P3–P5 cyclized macrocycles (see Experimental Section). These examples reveal a superior binding affinity for BIR2 and BIR3 than P2–P5 cyclized compounds (see Table 2). For example, a P3–P5 linked macrocycle (8) with *L*-valine in the P2 position and *L*-phenylalanine in the P4 position gave micromolar affinity for BIR2 and has an IC_{50} of 110 nM for BIR3. This compound was cocrystallized with the BIR2 domain, and when superimposed on the open chain, analogue 7 shows remarkable overlap of binding epitopes, supporting the proposed P3 to P5 macrocycle design. (Figure 2b).

8 was cyclized by reaction of the P3 azidoproline with the acetylene in a pent-4-ynoyl derivative of *L*-4-aminophenylalanine at P5. Inverting P5 stereochemistry (effectively only inversion of the carboxylic acid configuration, 9) had marginal effect on BIR3 affinity but a significant reduction in BIR2 affinity, suggesting the importance of a suitably oriented carboxylic acid. Other P5 substituents such as that derived from the Huisgen cyclization with *O*-propargyl-*L*-tyrosine (10) revealed good balanced affinity against XIAP BIR2 and BIR3, with IC_{50} values of 139 and 160 nM, respectively. Additionally, both 8 and 10 were shown to potentially

Table 2. Chemical Structures of P3–P5 Linked Macrocylic Compounds and Their Competitive Binding Affinities (IC_{50} Values) for XIAP BIR2 and BIR3 Domains, cIAP1 BIR3 Domain, and Activity in a Cell-Free Caspase-3 Rescue Assay



Cpd	HOOC-CH(NH ₂)-P2	P4	HOOC-CH(NH)-P5	XIAP BIR2 IC_{50} (μ M)	XIAP BIR3 IC_{50} (μ M)	cIAP1 BIR3 IC_{50} (μ M)	Caspase-3 rescue EC_{50} (μ M)
8	L-Val	phenyl		1.97	0.110	0.036	6.70
9	L-Val	phenyl		>18.8	0.232	-	-
10	L-Val	phenyl		0.139	0.160	0.020	1.40
11	L-cyclohexyl Gly	2-naphthyl		2.27	0.235	-	-
12	L ¹ BuGly	2-naphthyl		0.827	0.214	-	-

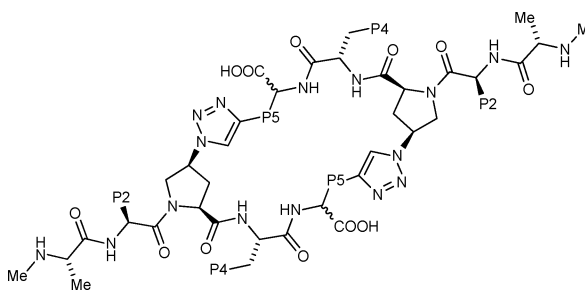
bind cIAP1 BIR3 with IC_{50} values 3–8-fold lower than XIAP BIR3 in FPA assays.

Functional Caspase-3 Rescue Assay. Having discovered macrocycles with potent binding to both XIAP BIR2 and BIR3 domains, it was important to demonstrate that the compounds also had functional activity. Specifically, by binding to the BIR2 and BIR3 domain, activated caspase-3 should be rescued. By determining the release of activated caspase-3 in a tumor cell lysate in the presence of recombinant XIAP BIR2–3 protein, it was possible to test the functional activity of macrocycles that bind to both BIR domains. Two P3–P5 linked macrocycles **8** and **10** were assessed in the caspase-3 rescue assay and exhibited EC_{50} values of 6.7 and 1.4 μ M, respectively (Table 2). Unfortunately, in each case, the functional activity was weaker than required for advancement.

Dimeric P3–P5 Macrocycles. The BIR2 and BIR3 binding domains exist in close proximity on the XIAP protein structure, and given that our objective was to develop a compound with affinity for both binding sites, we examined the possibility of introducing two binding epitopes into our macrocyclic inhibitors. Although a range of dimeric topologies might be envisioned, we focused exclusively on making macrocycles that constituted a head to tail dimerization of the P3–P5 linked monomeric macrocycles. Indeed, bivalent nonmacrocylic XIAP inhibitors have been described and their high potency has been attributed to hypervalency and possibly making simultaneous interactions with both binding domains.^{13,24–27} There are also reports of bivalent macrocyclic inhibitors,^{28,29} although these examples are structurally distinct from our series by being linked from the P2 side chain to the P4 position. They show very different binding activities for the BIR2 and BIR3 domains, with affinity for BIR2 generally weak and in the micromolar range. In contrast, our goal was to find compounds with equivalent inhibitory affinity for both BIR domains in the nM potency range.

Our strategy was to prepare the bivalent macrocycles for several of the best P3–P5 monomeric macrocycles (Table 3).

Table 3. Chemical Structures of P3–P5 Linked Dimeric Macrocylic Compounds and Binding Affinities for XIAP BIR2, BIR3, and cIAP1 BIR3



Cpd	HOOC-CH(NH ₂)-P2	P4	HOOC-CH(NH)-P5	XIAP BIR2 IC_{50} (μ M)	XIAP BIR3 IC_{50} (μ M)	cIAP1 BIR3 IC_{50} (μ M)
13	L-Val	phenyl		0.006	0.047	0.008
14	L-Val	phenyl		0.003	0.068	0.011
15	L-Val	1-naphthyl		0.219	0.029	0.017
16	L-Val	2-naphthyl		0.333	0.040	0.017
17	L-cyclohexyl Gly	2-naphthyl		0.740	0.054	0.024
18	L ¹ BuGly	2-naphthyl		0.097	0.036	0.016
19	L-Val	2-naphthyl		0.300	0.065	0.010

Generally, the dimeric material was synthesized as a byproduct of the solid supported synthesis of the monomeric compound (see Experimental Section), but yields of the dimer could be enhanced by employing a higher substitution density in the solid-phase synthesis, resulting in enhanced intermolecular reaction at the expense of intramolecular cyclization. On screening the dimeric macrocycles for binding affinity to XIAP BIR2 and BIR3 domains, we observed a significant enhancement in activity against both domains with, in many cases, similar affinities for each domain. For example, the dimeric macrocycle **14** has IC_{50} values of 3 nM against BIR2 and 68 nM against BIR3, a 46-fold (BIR2) and 2.4-fold (BIR3) improvement over the corresponding monomeric macrocycle (**10**), representing a ligand with unprecedented affinity for each of these domains. These dimers were also potent cIAP1 BIR3 binders.

Antiproliferative Cell Assay. The objective in designing and preparing potent inhibitors of the BIR2 and BIR3 domains was to find compounds that can significantly enhance cellular antiproliferative activity. Compounds proven to be functionally active in the caspase-3 rescue assay were progressed to whole cell antiproliferative assays in order to determine their ability to

inhibit cell growth in type I MDA-MB-231 (human triple negative breast cancer) and type II A875 melanoma cell-lines.

The caspase-3 rescue assay and tumor cell line antiproliferative data for key P3–P5 linked macrocycles, both monomeric and dimeric, is given in Table 4. The monomeric macrocycle **10** with

Table 4. Activity of Compounds in Caspase-3 Rescue and Antiproliferation Assays

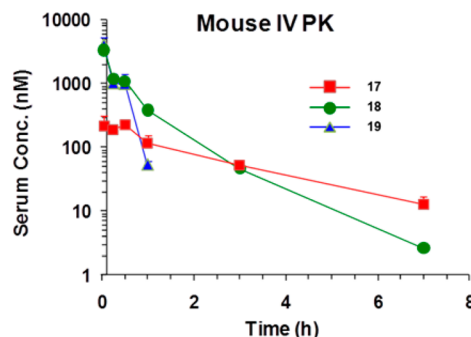
compd	XIAP BIR2–3 IC ₅₀ (μM)	cIAP1 BIR2–3 IC ₅₀ (μM)	caspase-3 rescue EC ₅₀ (μM)	MDA-MB- 231 cells IC ₅₀ (μM)	A875 cells IC ₅₀ (μM)
10			1.40	12.5	>10
13			0.070	7.90	
14			0.045	2.94	4.22
15			0.034	0.197	0.422
16			0.059	0.082	0.218
17	0.024	0.007	0.054	0.014	0.084
18	0.022	0.005	0.030	0.026	0.077
19	0.009	0.003	0.049	2.01	6.14

potent cIAP1 BIR3 activity but moderate XIAP BIR domain affinity and weak activity in the caspase-3 rescue assay showed weak antiproliferative effects in the type I MDA-MB-231 cell line and no measurable effect on the proliferation of the A875 type II cell line. The corresponding dimeric macrocycle **14** had significantly enhanced affinity for the XIAP BIR2 domain, and this translated into good caspase-3 rescue activity and measurable but weak antiproliferative activity in both type I and II cell lines despite potent cIAP1 BIR3 activity. Related dimeric macrocycles (e.g., **13**) similarly were disappointing in their antiproliferative activities despite (in some cases) good BIR domain binding and caspase-3 rescue activity. Overall, we attributed the weak antiproliferative activity to poor cell penetration for these large molecules.

There has been considerable investigation of cell membrane permeability for macrocyclic peptides and peptidomimetics that lie outside of Lipinski space.³⁰ As our compounds might have been too polar for good passive permeability, we synthesized analogues expected to have higher lipophilicity, within the SAR constraints for BIR2 and BIR3. Changes were structurally modest, for example, replacing the P2 side chain with *tert*-butyl and introducing naphthyl side chains into P4. The dimeric macrocycles prepared by these modifications had interesting activities. For example, **15** and **16** retain L-valine in the P2 position but have L-1- and L-2-naphthylalanine respectively in P4. Compared with **14**, this structural change has little effect on the caspase-3 rescue efficacy (despite a significant reduction in BIR2 inhibitory affinity), but a profound effect on antiproliferative properties. Both **15** and **16** have good activity against the type I cancer cell lines, and we observed sub-μM IC₅₀ values against type II A875 cells. More benefit was observed with L-cyclohexylglycine (**17**) or L-*tert*-butylglycine (**18**) in P2 while retaining L-2-naphthylalanine in P4. Potent binding affinity of these compounds for BIR2 and 3 domains translated into inhibition of both XIAP and cIAP1 BIR2–3 constructs tested in a FPA format. Caspase-3 rescue potency again was maintained, but antiproliferative activity was found with sub-100 nM IC₅₀ values. Screening in an antiproliferative assay with A549 cells (insensitive to a panel of known LAP antagonists) revealed IC₅₀ values above 25 μM, confirming that this is not a nonspecific cytotoxic effect (data not shown).

Pharmacokinetic Profiling. Selecting from among the more potent dimeric P3–P5 linked macrocycle inhibitors of XIAP, the

pharmacokinetic profiles of key compounds following iv administration in mice were investigated. Three potent macrocycles (**17**, **18**, and **19**) were administered iv to mice and blood levels of parent compound monitored. Plasma levels and pharmacokinetic parameters for these compounds are given in Figure 3. The results indicate that in general these macrocycles



Cpd	Dose (mg/kg)	T _{half} (h)	MRT (h)	Cl (mL/min/kg)	V _{ss} (L/kg)	AUC _{last} (mg/L·h)
17	0.2	1.9	2.5	4.4	0.7	457.2
18	1.0	0.85	0.79	7.1	0.34	1551.9
19	1.0	0.16	0.25	12.2	0.18	1072.3

Figure 3. Plasma levels and pharmacokinetic parameters for macrocycles **17–19** following intravenous administration to mice (**17** at 0.2 mg/kg, **18–19** both at 1 mg/kg).

have very low levels of clearance and low volumes of distribution, resulting in modest half-lives and mean residence times.

Human Tumor Xenograft Model in Mice. Because of its higher initial plasma concentrations and high overall exposure as determined by the AUC, **18** was evaluated for antitumor efficacy in the MDA-MB-231 human breast (Figure 4a) and A875 human melanoma (Figure 4b) xenograft models. An active result in these studies is defined as greater than 50% tumor growth inhibition (TGI) over at least one tumor volume doubling time (see Supporting Information (SI)). The macrocycle was administered by intraperitoneal injection (ip) every 3 days for a total of 5 administrations (q3d × 5) to nude mice bearing tumors staged to 100–150 mm³.

As shown in Figure 4a, **18** was inactive in the MDA-MB-231 model at 5 and 20 mg/kg, however, administration of the macrocycle at 50 mg/kg resulted in tumor growth inhibition of 78%. No overt toxicity (morbidity or weight loss) was observed with this macrocycle at any dose level throughout the dosing regimen. Interestingly, robust *in vivo* efficacy (148% TGI) was observed with **18** in the A875 model. Figure 4b illustrates the tumor regressions obtained during the dosing regimen, which lasted for 12 days after the last dose (day 34). A minimum effective dose was not established in this study.

CONCLUSION

Simultaneous inhibition of both cIAP BIR3 and caspase-binding BIR2/BIR3 domains in XIAP appears to be an effective way of inducing apoptosis and subsequently shrinking tumors in animal models of cancer. We have demonstrated that making libraries by DPC is an efficient way to discover novel macrocyclic XIAP inhibitors with associated SAR. We have used X-ray cocrystal structures to gain insights that resulted in modified macrocycle scaffolds with improved BIR domain binding. We also demonstrated that larger dimeric macrocycles containing two binding epitopes have significant functional activity in a caspase-3

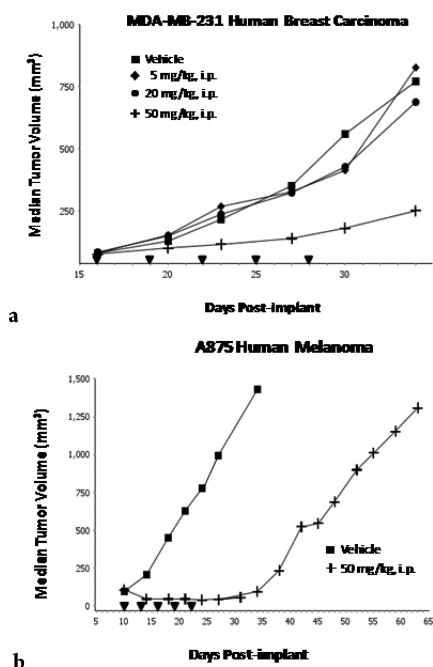


Figure 4. (a) Antitumor activity of **18** against established MDA-MB-231 human breast carcinoma xenografts implanted subcutaneously in athymic mice. Arrowheads indicate time of dosing (q3d \times 5). (b) Antitumor activity of **18** against established A875 human melanoma xenografts implanted subcutaneously in athymic mice. Arrowheads indicate time of dosing (q3d \times 5).

rescue assay. Through a rational modification of structure to enhance cell membrane permeability, we identified compounds with potent antiproliferative activity in both type I and type II cancer cell lines. Finally, a key dimeric macrocyclic IAP antagonist provided high exposures following iv administration in mice and good efficacy in a human xenograft tumor model, providing a basis for further exploration of macrocyclic IAP inhibitors.

EXPERIMENTAL SECTION

Macrocycle Library Synthesis. ELC libraries of macrocycles were made from commercially available components using the method previously described.²² Ring closure of the linear precursor mixtures covalently attached to DNA was achieved by copper(I)-catalyzed 1,2,3-triazole formation.

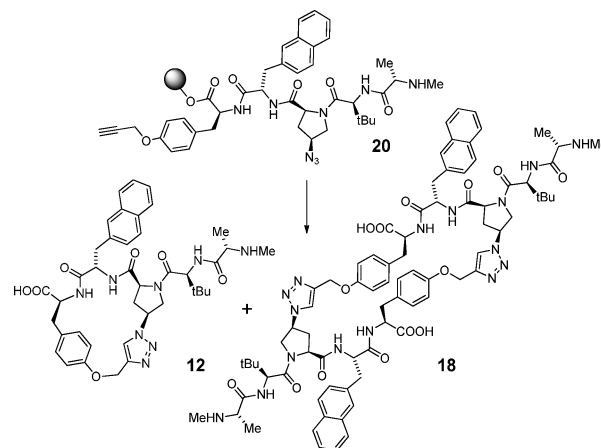
Individual Macrocycle Synthesis. Detailed experimental, purification details, proton NMR, HPLC, and MS data are provided in the SI. Purity of all final compounds was shown by HPLC to be $\geq 95\%$.

Linear precursors (e.g., **20**) were built using standard Fmoc amino acid chemistry on a Prelude parallel peptide synthesizer (Protein Technology, Tucson, AZ). Monomeric and dimeric macrocycles were obtained by the following general ring closure reaction illustrating the preparation of **18**.

A freshly made solution of copper(II) (*Z*)-2,2,6,6-tetramethyl-5-oxohept-3-en-3-olate (0.5 equiv), ascorbic acid (3 equiv), DIPEA (10 equiv), and 2,6-dimethylpyridine (10 equiv) in a solution of DMF and THF (1:1 v/v, 0.042 M) was added to the linear precursor **20** immobilized on resin support. The reaction mixture was agitated by a gentle stream of nitrogen for 30 min. The reagents were drained from the reaction vessel, and the resin was washed with DMF (6 \times 30 s per wash) and dichloromethane (6 \times 30 s per wash) and then deprotected and cleaved from the resin with 5% trifluoroacetic acid (TFA) in dichloromethane (5 min wash with cleavage solution, followed by a 30 s wash with cleavage solution, repeated twice). Solvent was removed in vacuo, and the crude reaction products formed a thick oil.

Separation of monomeric and dimeric macrocycles during the Cu²⁺-catalyzed cyclization was achieved on a Gilson HPLC containing a GX

281 liquid handler, UV/vis 155 detector at 220 and 254 nm, and a 321 pump (Gilson, Inc., Middleton, WI, USA) running at 20 mL/min with an Waters Xterra Prep MS C8, 5 μ m, 19 mm \times 100 mm column PN 186001935 (Waters Corporation, Milford, MA USA), using a solvent gradient from 5% acetonitrile (ACN)/water with 0.1% TFA increasing to 35% ACN/water with 0.1% TFA, followed by a rapid column flush with 100% ACN/water with 0.1% TFA.



Macrocycles **12** and **18** were obtained as a white powders following lyophilization. **12**: HRMS found 753.3720, C₈₀H₉₆N₁₆O₁₄ requires 753.3719. **18**: ¹H NMR (400 MHz, DMSO-*d*₆) δ 12.88 (2H, br s), 8.80 (4H, br s), 8.58 (2H, d, *J* = 8.0 Hz), 8.50 (2H, d, *J* = 8.0 Hz), 8.40 (2H, s), 8.21 (2H, d, *J* = 9.2 Hz), 7.87–7.82 (6H, m), 7.75 (2H, d, *J* = 8.4 Hz), 7.47–7.43 (6H, m), 7.16 (4H, d, *J* = 8.8 Hz), 6.81 (2H, d, *J* = 8.4 Hz), 5.25–5.16 (2H, m), 4.85 (2H, d, *J* = 11.6 Hz), 4.81 (2H, d, *J* = 11.6 Hz), 4.75 (2H, dd, *J* = 6.4, 13.2 Hz), 4.58–4.37 (10H, m), 4.47–4.37 (4H, m), 3.94 (2H, q, *J* = 6.0 Hz), 3.78 (2H, t, *J* = 5.6 Hz), 3.22–3.17 (2H, m), 3.06–3.03 (4H, m), 2.82–2.76 (4H, m), 2.32–2.21 (2H, m), 2.88 (6H, d, *J* = 6.8 Hz), 1.01 (18H, s). *m/z* 1506 ([M + 2H]²⁺). HRMS found 1505.7387, C₈₀H₉₆N₁₆O₁₄ requires 1505.7365. The compound was observed in the second charge state.

ASSOCIATED CONTENT

Supporting Information

Procedures for cocrystal structure determination, IAP binding assays, caspase-3 rescue assays, A875 cellular proliferation assays, pharmacokinetic and in vivo efficacy experiments, experimental procedures for the synthesis of all new building blocks, and spectroscopic data on final macrocycles. This material is available free of charge via the Internet at <http://pubs.acs.org>.

AUTHOR INFORMATION

Corresponding Author

*Phone: (617) 492-6977. Email: nterrett@ensembletx.com.

Author Contributions

All authors have given approval to the final version of the manuscript.

Notes

The authors declare no competing financial interest.

ACKNOWLEDGMENTS

We thank Celia D'Arienzo, Jinping Gan, Kevin Stefanski, Yuwei Tang, Ragini Vuppugalla, and Haiqing Wang for their assistance in obtaining the PK data for compound **18**.

ABBREVIATIONS USED

BIR, baculovirus inhibitor of apoptosis repeat; cIAP, cellular inhibitor of apoptosis; CL, clearance; DIPEA, diisopropyl-

ethylamine; DPC, DNA-programmed chemistry; EDCI, N-(3-(dimethylamino)propyl)-N-ethylcarbodiimide hydrochloride; FPA, fluorescence polarization assay; IAP, inhibitor of apoptosis protein; PCD, programmed cell death; SM, smac mimetic; Smac, second mitochondria-derived activator of caspases; TBST, tribuffered saline and Tween 20; TGI, tumor growth inhibition; V_{ss} , steady-state volume of distribution; XIAP, X-linked inhibitor of apoptosis protein

REFERENCES

- (1) Hanahan, D.; Weinberg, R. A. Hallmarks of cancer: the next generation. *Cell* **2011**, *144*, 646–674.
- (2) Earnshaw, W. C.; Martins, L. M.; Kaufmann, S. H. Mammalian caspases: structure, activation, substrates, and functions during apoptosis. *Annu. Rev. Biochem.* **1999**, *68*, 383–424.
- (3) Chang, H. Y.; Yang, X. Proteases for cell suicide: functions and regulation of caspases. *Microbiol. Mol. Biol. Rev.* **2000**, *64*, 821–846.
- (4) Wei, Y.; Fan, T.; Yu, M. Inhibitor of apoptosis proteins and apoptosis. *Acta Biochim. Biophys. Sin.* **2008**, *40*, 278–288.
- (5) Wilkinson, J. C.; Cepero, E.; Boise, L. H.; Duckett, C. S. Upstream regulatory role for XIAP in receptor-mediated apoptosis. *Mol. Cell. Biol.* **2004**, *24*, 7003–7014.
- (6) Srinivasula, S. M.; Ashwell, J. D. IAPs: What's in a Name? *Mol. Cell* **2008**, *30*, 123–135.
- (7) Eckelman, B. P.; Salvesen, G. S. The human anti-apoptotic proteins cIAP1 and cIAP2 bind but do not inhibit caspases. *J. Biol. Chem.* **2006**, *281*, 3254–3260.
- (8) Liu, Z.; Sun, C.; Olejniczak, E. T.; Meadows, R. P.; Betz, S. F.; Oost, T.; Herrmann, J.; Wu, J. C.; Fesik, S. W. Structural basis for binding of Smac/DIABLO to the XIAP BIR3 domain. *Nature* **2000**, *408*, 1004–1008.
- (9) Cai, Q.; Sun, H.; Peng, Y.; Lu, J.; Nikolovska-Coleska, Z.; McEachern, D.; Liu, L.; Qiu, S.; Yang, C. Y.; Miller, R.; Yi, H.; Zhang, T.; Sun, D.; Kang, S.; Guo, M.; Leopold, L.; Yang, D.; Wang, S. A potent and orally active antagonist (SM-406/AT-406) of multiple inhibitor of apoptosis proteins (IAPs) in clinical development for cancer treatment. *J. Med. Chem.* **2011**, *54*, 2714–2726.
- (10) Fulda, S. Molecular pathways: targeting inhibitor of apoptosis proteins in cancer—from molecular mechanism to therapeutic application. *Clin. Cancer Res.* **2014**, *20*, 289–295.
- (11) Flygare, J. A.; Beresini, M.; Budha, N.; Chan, H.; Chan, I. T.; Cheeti, S.; Cohen, F.; Deshayes, K.; Doerner, K.; Eckhardt, S. G.; Elliott, L. O.; Feng, B.; Franklin, M. C.; Reisner, S. F.; Gazzard, L.; Halladay, J.; Hymowitz, S. G.; La, H.; LoRusso, P.; Maurer, B.; Murray, L.; Plise, E.; Quan, C.; Stephan, J.-P.; Young, S. G.; Tom, J.; Tsui, V.; Um, J.; Varfolomeev, E.; Vucic, D.; Wagner, A. J.; Wallweber, H. J. A.; Wang, L.; Ware, J.; Wen, Z.; Wong, H.; Wong, J. M.; Wong, M.; Wong, S.; Yu, R.; Zobel, K.; Fairbrother, W. J. Discovery of a potent small-molecule antagonist of inhibitor of apoptosis (IAP) proteins and clinical candidate for the treatment of cancer (GDC-0152). *J. Med. Chem.* **2012**, *55*, 4101–4113.
- (12) Sun, H.; Lu, J.; Liu, L.; Yang, C. Y.; Wang, S. Potent and selective small-molecule inhibitors of cIAP1/2 proteins reveal that the binding of Smac Mimetics to XIAP BIR3 is not required for their effective induction of cell death in tumor cells. *ACS Chem. Biol.* **2014**, *18*, 994–1002.
- (13) Deveraux, Q. L.; Reed, J. C. IAP family proteins—suppressors of apoptosis. *Genes Dev.* **1999**, *13*, 239–252.
- (14) Vogler, M.; Walczak, H.; Stadel, D.; Haas, T. L.; Genze, F.; Jovanovic, M.; Gschwend, J. E.; Simmet, T.; Debatin, K. M.; Fulda, S. Targeting XIAP bypasses Bcl-2-mediated resistance to TRAIL and cooperates with TRAIL to suppress pancreatic cancer growth in vitro and in vivo. *Cancer Res.* **2008**, *68*, 7956–7965.
- (15) Condon, S. M.; Mitsunuchi, Y.; Deng, Y.; LaPorte, M. G.; Rippin, S. R.; Haimowitz, T.; Alexander, M. D.; Kumar, P. T.; Hendi, M. S.; Lee, Y.-H.; Benetatos, C. A.; Yu, G.; Kapoor, G. S.; Neiman, E.; Seipel, M. E.; Burns, J. M.; Graham, M. A.; McKinlay, M. A.; Li, X.; Wang, J.; Shi, Y.; Feltham, R.; Bettjeman, B.; Cumming, M. H.; Vince, J. E.; Khan, N.; Silke, J.; Day, C. L.; Chunduru, S. K. Birinapant—A Smac-mimetic with improved tolerability for the treatment of solid tumors and hematological malignancies. *J. Med. Chem.* **2014**, *57*, 3666–3677.
- (16) Galbán, S.; Hwang, C.; Rumble, J. M.; Oetjen, K. A.; Wright, C. W.; Boudreaux, A.; Durkin, J.; Gillard, J. W.; Jaquith, J. B.; Morris, S. J.; Duckett, C. S. Cytoprotective effects of IAPs revealed by a small molecule antagonist. *Biochem. J.* **2009**, *417*, 765–771.
- (17) Hennessy, E. J.; Adam, A.; Aquila, B. M.; Castriotta, L. M.; Cook, D.; Hattersley, M.; Hird, A. W.; Huntington, C.; Kamhi, V. M.; Laing, N. M.; Li, D.; MacIntyre, T.; Omer, C. A.; Oza, V.; Patterson, T.; Repik, G.; Rooney, M. T.; Saeh, J. C.; Sha, L.; Vasbinder, M. M.; Wang, H.; Whitston, D. Discovery of a novel class of dimeric Smac mimetics as potent IAP antagonists resulting in a clinical candidate for the treatment of cancer (AZD5582). *J. Med. Chem.* **2013**, *56*, 9897–9919.
- (18) Driggers, E. M.; Hale, S. P.; Lee, J.; Terrett, N. K. The exploration of macrocycles for drug discovery—an underexploited structural class. *Nature Rev. Drug Discovery* **2008**, *7*, 608–624.
- (19) Gartner, Z. J.; Liu, D. R. The generality of DNA-templated synthesis as a basis for evolving non-natural small molecules. *J. Am. Chem. Soc.* **2001**, *123*, 6961–6963.
- (20) Gartner, Z. J.; Kanan, M. W.; Liu, D. R. Multistep small-molecule synthesis programmed by DNA templates. *J. Am. Chem. Soc.* **2002**, *124*, 10304–10306.
- (21) Gartner, Z. J.; Tse, B. N.; Grubina, R.; Doyon, J. B.; Snyder, T. M.; Liu, D. R. DNA-templated organic synthesis and selection of a library of macrocycles. *Science* **2004**, *305*, 1601–1605.
- (22) Kleiner, R. E.; Dumelin, C. E.; Liu, D. R. Small-molecule discovery from DNA-encoded chemical libraries. *Chem. Soc. Rev.* **2011**, *40*, 5707–5717.
- (23) Tsantrizos, Y. S.; Bolger, G.; Bonneau, P.; Cameron, D. R.; Goudreau, N.; Kukolj, G.; LaPlante, S. R.; Llinàs-Brunet, M.; Nar, H.; Lamarre, D. Macrocyclic inhibitors of the NS3 protease as potential therapeutic agents of hepatitis C virus infection. *Angew. Chem., Int. Ed.* **2003**, *42*, 1356–1360.
- (24) Li, L.; Thomas, R. M.; Suzuki, H.; De Brabander, J. K.; Wang, X.; Harran, P. G. A small molecule Smac mimic potentiates TRAIL- and TNF α -mediated cell death. *Science* **2004**, *305*, 1471–1474.
- (25) Sheng, R.; Sun, H.; Liu, L.; Lu, J.; McEachern, D.; Wang, G.; Wen, J.; Min, P.; Du, Z.; Lu, H.; Kang, S.; Guo, M.; Yang, D.; Wang, S. A potent bivalent Smac mimetic (SM-1200) achieving rapid, complete, and durable tumor regression in mice. *J. Med. Chem.* **2013**, *56*, 3969–3979.
- (26) Sun, H.; Nikolovska-Coleska, Z.; Lu, J.; Meagher, J. L.; Yang, C. Y.; Qiu, S.; Tomita, Y.; Ueda, Y.; Jiang, S.; Krajewski, K.; Roller, P. P.; Stuckey, J. A.; Wang, S. Design, synthesis, and characterization of a potent, nonpeptide, cell-permeable, bivalent Smac mimetic that concurrently targets both the BIR2 and BIR3 domains in XIAP. *J. Am. Chem. Soc.* **2007**, *129*, 15279–15294.
- (27) Nikolovska-Coleska, Z.; Meagher, J. L.; Jiang, S.; Kawamoto, S. A.; Gao, W.; Yi, H.; Qin, D.; Roller, P. P.; Stuckey, J. A.; Wang, S. Design and characterization of bivalent Smac-based peptides as antagonists of XIAP and development and validation of a fluorescence polarization assay for XIAP containing both BIR2 and BIR3 domains. *Anal. Biochem.* **2008**, *374*, 87–98.
- (28) Nikolovska-Coleska, Z.; Meagher, J. L.; Jiang, S.; Yang, C. Y.; Qiu, S.; Roller, P. P.; Stuckey, J. A.; Wang, S. Interaction of a cyclic, bivalent smac mimetic with the x-linked inhibitor of apoptosis protein. *Biochemistry* **2008**, *47*, 9811–982.
- (29) Sun, H.; Liu, L.; Lu, J.; Qiu, S.; Yang, C. Y.; Yi, H.; Wang, S. Cyclopeptide Smac mimetics as antagonists of IAP proteins. *Bioorg. Med. Chem. Lett.* **2010**, *20*, 3043–3046.
- (30) Rezaei, T.; Yu, B.; Millhauser, G. L.; Jacobson, M. P.; Lokey, R. S. Testing the conformational hypothesis of passive membrane permeability using synthetic cyclic peptide diastereomers. *J. Am. Chem. Soc.* **2006**, *128*, 2510–2511.